

## HOW TO ACHIEVE REGULAR SEISMIC BEHAVIOR OF IRREGULAR BRIDGES WITH UNEQUAL HEIGHT PIERS?

Mena. G. Ishak<sup>1\*</sup>, Sameh. S.F. Mehanny<sup>2</sup>

<sup>1\*</sup> Bridge Design Engineer, Dar Al-Handasah, Smart Village, Egypt

& M.Sc. Graduate student, Cairo University, Egypt

[Mena.Gerges@dargroup.com](mailto:Mena.Gerges@dargroup.com)

<sup>2</sup> Professor of Structural Engineering, Faculty of Engineering, Cairo University, Egypt

[sameh.mehanny@stanfordalumni.org](mailto:sameh.mehanny@stanfordalumni.org)

**Keywords:** Seismic Analysis, bridge regularity, inelastic analysis, unequal pier heights, EC8.

**Abstract.** EuroCode 8 simplistically addresses the seismic behavior of irregular bridges. The proposed criterion for regularizing the response depends on the ratio between the moment demand and moment capacity on each pier aiming to regularize the distribution of seismic design demand among, and ultimately guarantee synchronized failure of, all piers irrespective of their different heights. This criterion may not be effective in addressing some pier height ratios within the same bridge, hence results may not be as expected by code developers. The present paper scrutinizes and evaluates the validity of the criterion proposed by EC8, where the seismic response of four types (featuring a permutation of elastomeric and/or pot bearings along with monolithic pier-to-deck connections) of three-span continuous bridges with one short and one long pier designed to satisfy EC8 regularity condition are compared. Each bridge type has been investigated for four different pier height ratios. Several nonlinear static and dynamic analyses have been performed on each of the total sixteen schemes (namely, four pier height ratios for each of the four bridge types). Nonlinear analysis has resulted in different bridge behavior from that mentioned (and expected) by EC8. The study has led to evidence of realizing somehow regular seismic behavior by altering EC8-design obtained steel reinforcement ratios in either piers of each bridge scheme. It has been also noted that bridge regularity is achieved more efficiently in bridges with elastomeric bearings on shorter piers rather than bridges without elastomeric bearings.

\* The asterisk denotes the presenting author.

## 1. INTRODUCTION

Seismic behavior of bridges has been an important topic addressed in most codes and design references worldwide. EuroCode 8 [1 & 2] has demonstrated design guidelines for bridges under seismic loads, and one of these guidelines is determining bridge uniformity in order to estimate the actual bridge behavior when exposed to seismic loading. According to EC8 [1 & 2], bridges satisfying regularity criteria (namely, demonstrating  $\rho < 2$  as per Equation 1) are considered uniform; hence, reaching a value of  $\rho=1$  implicitly means that the bridge will have strictly uniform response and anticipated perfect synchronized failure of all its piers.

$$\rho = \frac{r_{\max}}{r_{\min}} < \rho_0 = 2, \text{ where } r = q \frac{M_{Edi}}{M_{Rdi}} \quad (1)$$

For bridges with uniform ductile behavior,  $q$  is assumed to have a value of 3.5 as per code recommendations,  $M_{Edi}$  is the design moment already reduced by the behavior factor  $q$ , and the value of  $M_{Rdi}$  is the resistance moment determined from moment curvature relation. Accordingly, strict uniformity of behavior should imply that all piers reach their  $M_{Rdi}$  values somehow simultaneously which leads to a value of  $\rho$  of approximately 1. Bridges violating the criterion of Equation (1) shall be designed in accordance to irregular behavior in the designated direction and hence, shall be designed with a reduced behavioral factor value (i.e.,  $q < 3.5$ ). EC8 regularity criteria can be modified as proposed herein where we can compare values of curvature demand to curvature capacity at critical sections in piers while computing  $r_{\max}$  and  $r_{\min}$  as per Equation 2 rather than moment in order to appropriately capture inelastic effects on the response. An enhanced regularity index,  $\rho_\phi$ , is then calculated using this improved curvature-based  $r$  values instead of the codified  $\rho$  index relying on moment-based  $r$  values.

$$r = \frac{\text{Curvature Demand of column, } \phi_{Edi}}{\text{Curvature Capacity of column, } \phi_{Rdi}} \quad (2)$$

Pushover analysis is performed in the present research adjacent to nonlinear dynamic analysis in order to provide accurate results for verifying EC8 regularity criteria. Building on a previous research effort by Guirguis and Mehanny (2012) [3], this paper further scrutinizes and evaluates the validity of the proposed code criterion for bridge uniformity and suggests effective, smart and economic means to provide uniform seismic response of apparently irregular bridges.

## 2. MODELING AND DESIGN

Implementing previous work in [3], our case study bridge consists of three equal spans with a total length of 84m (refer to figure 1) divided into four categories, all of which were designed according to EC8 thus satisfying uniformity condition ( $\rho < 2$ ) and hence anticipating somehow “near” synchronized behavior of unequal height piers. Each of the four categories has a pre-stressed deck with both ends resting on abutments connected to the bridge via sliding elastomeric bearings, while the two intermediate piers feature different pier-to-deck connections with various permutations as illustrated in table 1. Both piers are assumed to have equal dimensions regardless of the pier height despite the fact that perfect state material economy can be achieved through differentiating short and long pier cross-section dimensions for each bridge scheme. Such assumption is in line with previous researches in the literature

[4-6] that were largely focusing on piers with equal cross-section dimensions irrespective of their heights for aesthetical and practical – from constructability perspective – purposes.

Category / Piers Cross-section	Short Pier-to-Deck Connection (Height =7m, 9m, 10.5m & 12m)	Long Pier-to-Deck Connection (Height =14m)	Category Symbol
1 / 3.5m x 1.4m	non sliding Elastomeric bearing	non sliding Pot bearing	E-P
2 / 3.5m x 1.4m	non sliding Elastomeric bearing	Monolithic connection	E-M
3 / 3.5m x 1.8m	non sliding Pot bearing	Monolithic connection	P-M
4 / 3.5m x 1.8m	non sliding Pot bearing	non sliding Pot bearing	P-P

Table 1 – The sixteen case-study bridge schemes under investigation with categories description.

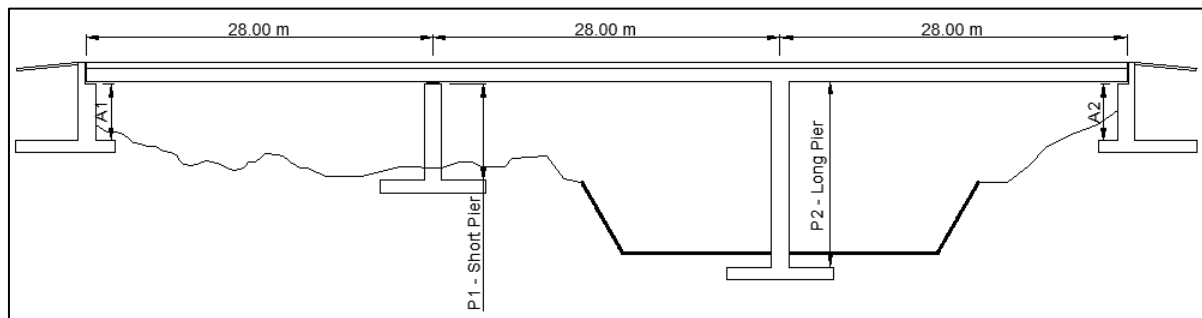


Figure 1a – Case Study Bridge General Arrangement

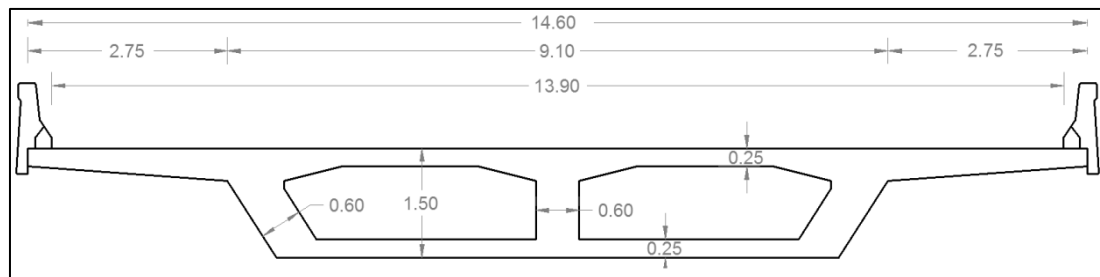


Figure 1b – Typical Bridge Deck Cross-section (dimensions in meters)

Static inelastic pushover and nonlinear dynamic analyses are performed on categories 1 and 2 using Opensees software [7], while only pushover analysis is performed on categories 3 and 4. Piers are assumed to have a fixed connection to the ground ignoring the effect of soil-structure interaction. Piers are modeled as fiber sections possessing two characteristic zones with different properties (confined zone and unconfined zone). Abutments featuring a gap of 200 mm to the deck are considered and modeled according to [8] after gap closure due to deck movement under seismic events. Accordingly, as a result of the movement of sliding elastomeric bearings on abutment's shelf closing the 200 mm gap to the abutment's back wall, passive earth pressure behind abutment is mobilized as shown in figure 2 and is considered in the model through an effective stiffness,  $K_{eff}$ .

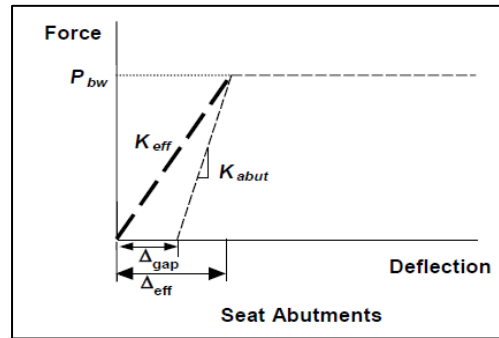


Figure 2 – Abutment effective stiffness after gap closure [8].

As stated above, concrete of the pier was utilized into two zones. The confined concrete zone has an expected compressive strength of 45 MPa, a characteristic ultimate compressive strain of 0.014 and no tensile strength, while the unconfined concrete zone possesses a nominal cylinder strength of 28 MPa, and an expected strength of 36 MPa ( $f'_{ce}=1.3 f'_c$ ). Reinforcing steel is modeled as uniaxial bilinear material and is characterized by initial elastic behavior with modulus of elasticity  $E_s=200\text{GPa}$ , followed by strain hardening region after reaching an expected yield stress  $f_y=475\text{MPa}$  and hardening modulus of 4.75 MPa, with a failure strain of 0.09. The usage of “expected” material properties while performing nonlinear inelastic analysis of the bridge up to collapse limit state is recommended rather than nominal (i.e., design) material properties to get a better estimate of the capacity of structural components. This assumption does not apply to shear for which we still rely on nominal material properties since shear leads to brittle failure. In the current study, piers capacity is assumed to be controlled by “axial-flexure” behavior and piers are hence not prone to shear failure. Furthermore, Fiber Section Analysis (FSA) is performed for piers where each bridge pier cross-section is divided into an array of confined and unconfined concrete and steel fibers according to the design requirements in order to generate moment-curvature capacity curves (refer to Fig. 3 for a sample) as well as to check relevant failure criteria (stated in a following section of the paper) at the material stress-strain level either for confined concrete or reinforcing bars.

Non-sliding pot bearings are modeled by simply introducing moment release at top of pier at its junction with the deck. On the other hand, non-sliding elastomeric bearings atop of pier are modeled primarily as an elastic material. Horizontal spring (in the deck longitudinal direction) modeling the shear stiffness of the elastomeric bearing is hence introduced and assigned a stiffness value that is equal to the shear modulus of the elastomer material,  $G_b$ , multiplied by the foot print area of the bearing,  $A_b$ , and divided by the total thickness of the elastomer,  $t_b$ . The shear stiffness of all elastomeric bearings supporting the deck (represented by a single spine in the current computational model) at the pier location is hence the stiffness of a single bearing estimated as above multiplied by their number,  $n$ . As per EN 1998-2 (2005) - Cl. 7.5.2.4 (5),  $G_b$  has been taken in the present research with the value proposed for short term (i.e., seismic) response as 1.485 MPa [ $G_b = 1.1 \times (1.15\text{MPa}+0.2\text{MPa})$ ]. Elastomeric bearings dimensions used were 550 mm x 500 mm with a total thickness of 150 mm. It has to be finally noted that the equivalent lateral stiffness of the “pier-elastomeric bearing” supporting system as captured by the model throughout the analysis is that of two springs in series: one of them corresponds to the elastomeric bearings themselves deforming in transverse shear mode, while the other corresponds to the pier lateral stiffness, and hence the combined stiffness is less than the least of the two values.

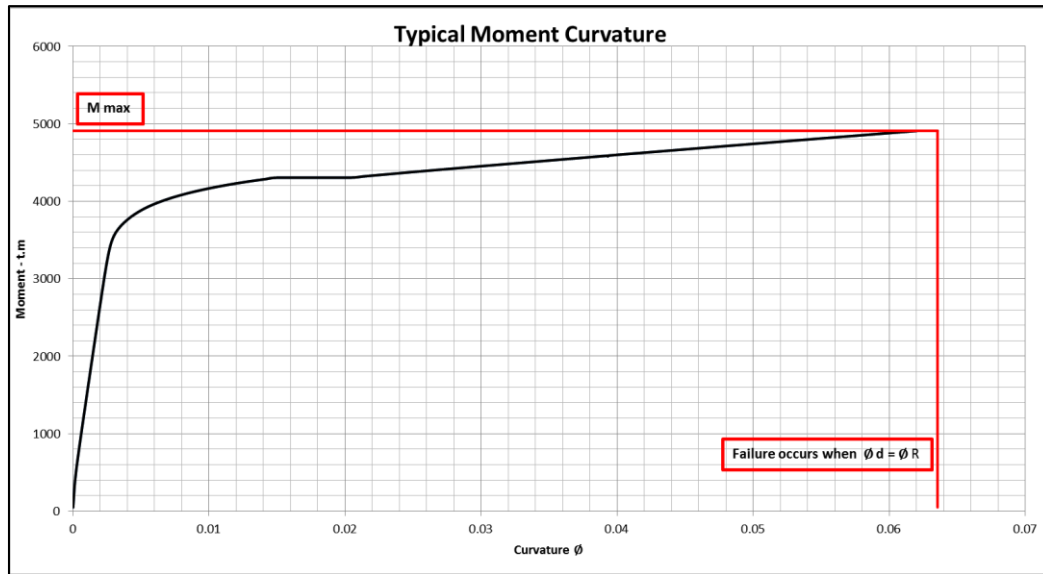


Figure 3 – Typical (sample) moment-curvature graph resulting from FSA.

A flow chart is implemented (figure 4) to organize the design hierarchy and provide systematic loop in order to converge results as possible to match research purpose. The cycle starts with designing the – on scope – bridge according to EC8. All bridges in this research satisfy EC8 regularity condition and other code recommendations. After that, pushover analysis is performed which in most cases show signs of irregularity, then a modification in steel reinforcement is performed –without violating code minimum requirements – in order to reach most possible regular behavior. Finally, a time history analysis is performed to confirm the analysis results from the pushover analysis.

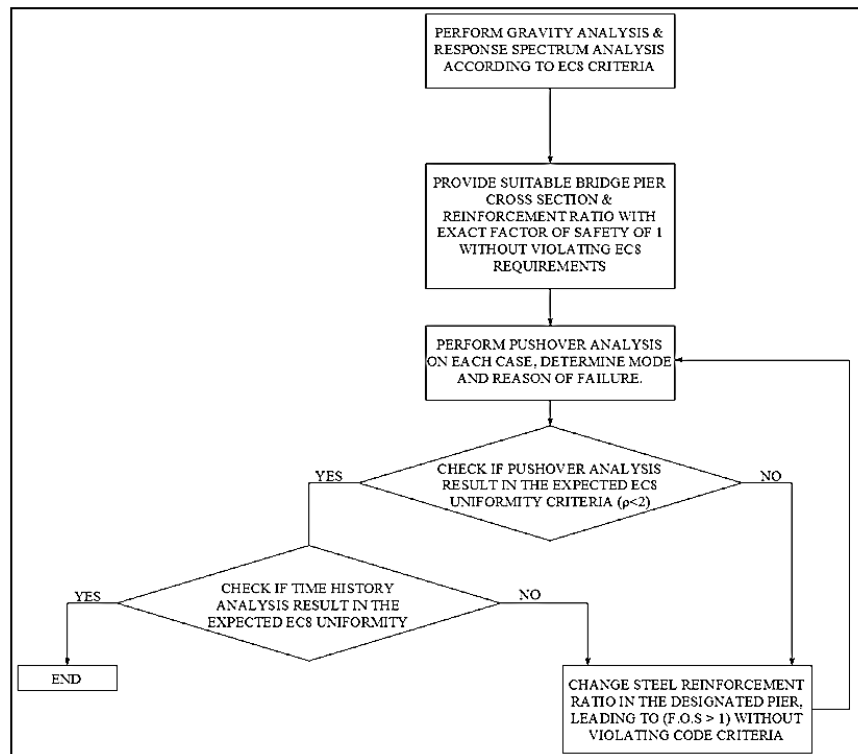


Figure 4 – Flow chart illustrating current research investigation (design/analysis) hierarchy.

### 3. FAILURE CRITERIA

Key failure criteria in this research are identified as whichever occurs first: a ductile mode of failure when steel reaches ultimate strain versus a brittle mode of failure when confined concrete reaches its ultimate strain. Bridge piers are considered to have reached their ultimate curvature when either outermost confined concrete fibers reach a strain of 0.014 or steel bars reach a strain of 0.09. However, for conservatism in predicting ductility capacity (and consequently curvature at failure) we could consider SCDOT (2008) [9] assumption that ultimate curvature of the piers cross section corresponds to the maximum moment the cross section can bear provided that neither of the above two conditions on material strains occurs prior to this. FSA plays a key role in determining the exact values of stress and strain in each partition of the critical section of the pier in order to identify the precise cause of failure.

Another modes of failure away from bridge piers that are further checked for completeness are (a) when a total longitudinal displacement of the bridge deck exceeds a given limiting displacement at abutment leading to deck falling off abutment ledge, and (b) when non sliding elastomeric bearings – whenever used atop of pier – reaches their maximum shear deformation. This maximum (limiting) lateral deformation within the bearing is specified herein as three times the elastomer thickness  $t_b$  and is assumed to demarcate “full” tearing of the elastomeric bearing based on scattered information gathered from experimental and analytical results in the literature [10 & 11]. However, this criterion by itself is not strictly marking a collapse state of the bridge as a whole. Total bridge failure will not happen unless there is an off-seating of the deck from the abutments’ shelves, i.e., maximum deck displacement exceeds off-seating limiting values. Hence, tearing of bearings without off-seating may be considered a “weak/soft” mode of failure that could be restored by bearing replacement [12] and therefore the bridge is further investigated in the present research after reaching this *weak* failure state.

#### 4. IMPLEMENTING EC8 UNIFORMITY CRITERIA ON CASE STUDY BRIDGES

Elastic analysis according to EC8 is performed in order to design the unequal height bridge piers cross sections. Response spectrum analysis is hence conducted for a ground acceleration  $a_g = 0.3g$  representing moderate to high seismicity, soil type B with the following relevant factors ( $S=1.2$ ,  $T_b=0.15$ ,  $T_c=0.5$ ,  $T_d=2$ ), and a high importance factor of 1.3; and the design of piers is carried out for a behavior factor  $q=3.5$  (ductile response) with pier effective inertia of 50% of pier gross inertia which was recommended in EN 1998-1 article 4.3.1. Table 2a summarizes the required steel percentage for each investigated bridge category and for each pier. A likely live load (20% of the total) is used in the seismic mass as well as in the seismic design load combination according to EC8 design requirements. The main concept followed herein in the piers design is to guarantee a factor of safety against flexure of exactly 1.0 relying on the generated “axial force-bending moment” interaction diagram for each pier and the design values retrieved from the elastic response spectrum analysis after being reduced by  $q$ . However, in order for all design scenarios generated in the current research to represent realistic cases that do not violate code rules, it has been decided to increase design-obtained reinforcement ratios in case they do not satisfy minimum reinforcement ratio determined as per EN 1992-1-1 (2004) - Cl. 9.5.2 [13] which has resulted in a factor of safety against flexure that is larger than 1.0 for these specific cases. This has been reflected in the values reported in table 2a. For completeness, table 2b converts reinforcement ratios given in table 2a into actual reinforcement steel tonnage to facilitate comparisons of the different design schemes.

Short pier Height	Cat 1 (E-P) 3.5m x 1.4m		Cat 2 (E-M) 3.5m x 1.4m		Cat 3 (P-M) 3.5m x 1.8m		Cat 4 (P-P) 3.5m x 1.8m	
	short	long	short	long	short	long	short	long
7m	0.200%	1.042%	0.200%	1.363%	1.780%	0.407%	1.880%	0.200%
9m	0.200%	1.077%	0.200%	1.403%	1.320%	0.661%	1.580%	0.405%
10.5m	0.250%	1.122%	0.200%	1.443%	1.060%	0.842%	1.270%	0.538%
12m	0.280%	1.128%	0.200%	1.443%	0.840%	0.966%	1.068%	0.686%

**Note:** minimum computed steel reinforcement ratio according to EC2 is 0.2%

Table 2a – Steel reinforcement ratios in piers of different investigated bridge categories as per design conforming to EC8 requirements (without steel reinforcement alterations for optimal uniform seismic response).

Short pier Height	Cat 1(E-P) 3.5m x 1.4m	Cat 2(E-M) 3.5m x 1.4m	Cat 3(P-M) 3.5m x 1.8m	Cat 4(P-P) 3.5m x 1.8m
7m	614	788	898	790
9m	649	825	1045	984
10.5m	706	857	1133	1032
12m	737	870	1167	1109

Table 2b – Steel reinforcement total weight (in tons) used in design version/trial 1

Table 3 summarizes the values of  $\rho$  computed as per Equation (1) for the different schemes reported in table 2. Referring to table 3, all  $\rho$  values appear to satisfy the regularity criteria (namely, demonstrating  $\rho < 2$ ) spelled out in EC8 and in most cases are even too close to a



value of 1 corresponding to perfect anticipated fully synchronized seismic behavior of unequal height piers up to failure. However, further investigation through nonlinear static and dynamic analysis shall be carried out in order for such conclusion of satisfying seismic response regularity to be either approved or denied.

It is nonetheless worth noting from table 3 that best uniform seismic behavior among unequal height piers for very short pier bridge schemes (namely, 7m- and 9m-high) is anticipated for category 2 ( $\rho$  is very close to 1.0) apparently followed by category 4, while best regular behavior for relatively long pier bridge schemes (namely, 10.5m- and 12m-high) is expected for categories 1, 2 and 4 ( $\rho$  is practically 1.0). However, detailed nonlinear analysis scrutinizing relative curvature demand-to-capacity ratios among piers up to failure – and not only looking into strength as suggested by code recommendations – is yet to be performed for validation of the seismic response regularity of the different categories.

Short pier Height	Cat 1(E-P) 3.5m x 1.4m	Cat 2(E-M) 3.5m x 1.4m	Cat 3(P-M) 3.5m x 1.8m	Cat 4(P-P) 3.5m x 1.8m
7m	1.235	1.010	1.624	1.087
9m	1.030	1.005	1.355	1.021
10.5m	1.013	1.016	1.251	1.007
12m	1.015	1.026	1.195	1.017

Table 3 - Values of  $\rho$  (Equation 1) for the sixteen investigated bridge schemes designed as per EC8 requirements

Moreover, despite that categories 4 and 3 as designed per EC8 recommendations may provide reliable seismic response similar to code compliant categories 1 and 2 (but not necessarily in terms of anticipated regularity in seismic behavior), one should realize that this is achieved at the expense of larger concrete dimensions of piers (and somehow generally higher reinforcement quantities); refer to table 2 and compare design data for category 1 versus category 4 and category 2 versus category 3.

## 5. PUSHOVER ANALYSIS AND DESIGN OPTIMISATION FOR REGULARIZED RESPONSE

Various design trials/alterations are performed starting from EC8 compliant designs (table 2) ending with most suitable version with reasonable steel reinforcement ratios to approach regularity (and synchronized failure of piers) as shown in table 4a. Version/trial 1 denotes pushover analysis performed on bridges with steel reinforcement according to EC8 design requirement as reported in table 2. Increasing either short or long pier steel reinforcement can lead to better uniformity in bridge behavior, where *perfect* uniform behavior is achieved when proposed  $\rho_\phi$  calculated at failure reaches a value of 1. It is noted that global bridge behavior approaches regularity whenever the difference between pier heights decreases. Altering steel reinforcement in short pier can improve uniformity in seismic response such as in categories 1, 2 and 4, while altering steel reinforcement in long pier in category 3 demonstrates better behavior in terms of uniformity. Steel reinforcement alteration applied herein does not violate EC8 recommendations (i.e. minimum or maximum steel reinforcement, etc.) but it also provides better performance and over strength (to be discussed in details later).



In case of category 1 bridges, it is noticed that investigated bridges start with design version 1 (EC8 compliant as per table 2) from a state far from regularity compared to categories 2, 3 & 4. This means that different pier-to-deck connections could affect the bridge uniformity drastically regardless of design requirements and recommendations. Category 2 bridges possess a better starting behavior than category 1 as demonstrated in figure 5, which is due to the fact that monolithic connection atop of the long pier provides better force redistribution among both piers than pot bearing pier-to-deck connection. Category 3 has a different trend in the behavior than the other versions as the steel reinforcement ratio in long piers rather than short piers is altered to target more uniform response at failure. It is noticed that this scheme may provide good solution in case of large difference between pier heights, while its benefits are diminished when the gap between both pier heights decreases, which then results in unpractical solution. A radically different behavior appears in category 4 starting from short pier height of 7m; it is impossible to reach reasonable values of regularity by just altering steel reinforcement ratios of the two piers. This is due to the fact that the stated EC8 design recommendation provides the most likely uniform behavior that could be achieved tied with the section minimum steel reinforcement requirement; if we can override this minimum reinforcement we can achieve better uniformity as noted in dashed lines in figure 5. This behavior further improves dramatically when short pier height increases from 7m to 9m but it is still away from regularity. The regularity/uniformity of response improves among pier heights of 10.5m and 12m but still no synchronization of failure of piers is achievable for this category of the case-study bridges.

As outlined above, the results obtained from pushover analysis showed a clear variation in seismic behavior among investigated categories. Thus, further nonlinear hysteretic time history analyses are performed herein on both “category 1” and “category 2” in order to validate the significance of the pushover analysis results. Time history analysis of categories 3 and 4 is still ongoing by the authors and results are not presented in this manuscript. Shown in table 4a are the optimal reinforcement ratios (retrieved through pushover analysis effort) that *more-or-less* satisfy regularity condition and that are considered throughout the time history analysis. Note the difference between these values in table 4a and those calculated by simply satisfying EC8 design requirements in table 2 without focusing on achieving regular seismic response of piers at failure. For completeness, table 4b converts these reinforcement ratios in table 4a of the optimized design for uniform seismic response into actual reinforcement steel tonnage to facilitate comparisons.

Short pier Height	Cat 1(E-P) 3.5m x 1.4m		Cat 2(E-M) 3.5m x 1.4m		Cat 3(P-M) 3.5m x 1.8m		Cat 4(P-P) 3.5m x 1.8m	
	short	long	short	long	short	long	short	long
7m	1.900 %	1.042%	1.000%	1.363%	1.780%	0.500%	1.880%	0.200%
9m	2.290%	1.077%	0.460%	1.403%	1.320%	1.100%	2.000%	0.405%
10.5m	2.000%	1.122%	0.400%	1.443%	1.060%	1.800%	1.880%	0.538%
12m	1.300%	1.128%	0.280%	1.443%	0.840%	2.000%	2.000%	0.686%

Table 4a – Steel reinforcement ratios used to comprehend best achievable uniform behavior (retrieved from pushover analysis successive trials)

Short pier Height	Cat 1(E-P) 3.5m x 1.4m	Cat 2(E-M) 3.5m x 1.4m	Cat 3(P-M) 3.5m x 1.8m	Cat 4(P-P) 3.5m x 1.8m
7m	1072	1003	962	790
9m	1373	915	1349	1171
10.5m	1412	939	1797	1348
12m	1208	906	1883	1662

Table 4b – Steel reinforcement total weight (in tons) for the two piers resulting from the optimized design

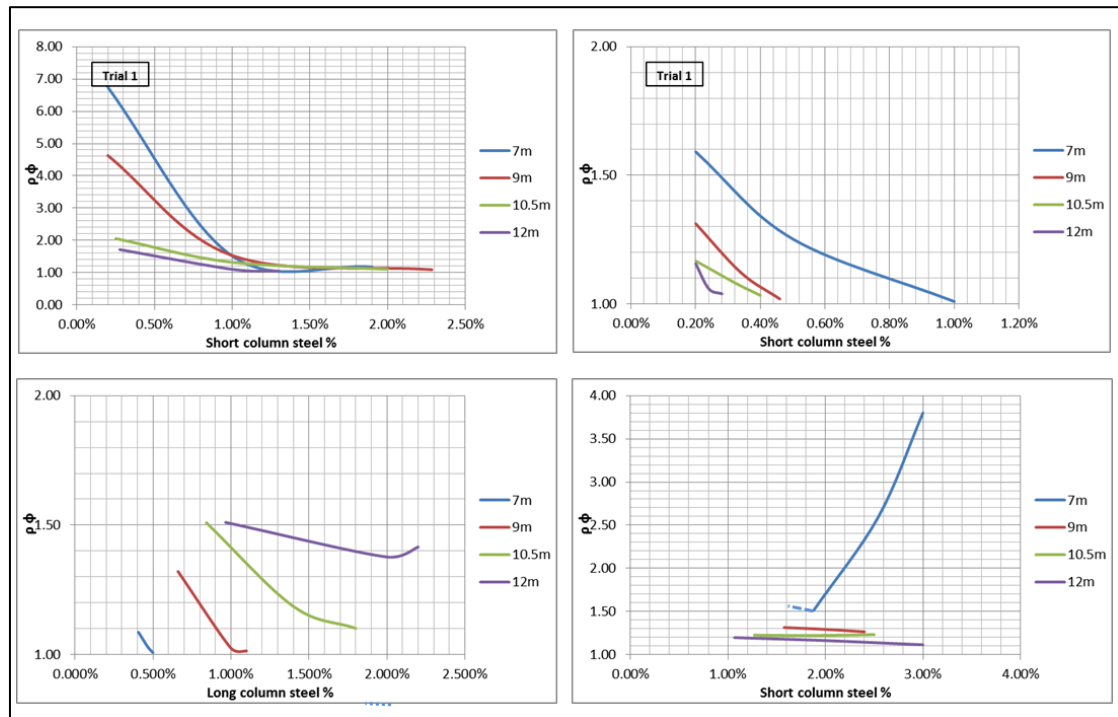
Figure 5 – Uniformity behavior from pushover analysis successive trials, top left: category 1, top right: category 2, bottom left: category 3, bottom right: category 4 [ $\rho_\phi$  values are calculated at failure state].

Table 5a reports  $\rho_\phi$  values computed for version (i.e., trial) 1 corresponding to EC8-based design without steel reinforcement alterations. Comparing EC8-calculated  $\rho$  values (as per Equation 1) in table 3 to proposed curvature-based  $\rho_\phi$  values in table 5a retrieved from pushover analysis at failure as specified above, one could notice that even when a bridge scheme complies with EC8 uniformity behavior it still has the possibility of acting somewhat non-uniform at failure limit state. For completeness, table 5b also reports  $\rho_\phi$  values at failure but for the bridge schemes featuring reinforcement ratios (table 4a) that have been optimized to attain *more-or-less* best regular response at failure based on pushover analysis results. It is hereby clear that categories 1 and 2 are capable of providing satisfactory uniform/regular seismic response at failure for all investigated pier height ratios while this is not strictly the case for all design schemes in categories 3 and 4 with various investigated pier height ratios.

Short pier Height	Cat 1(E-P) 3.5m x 1.4m	Cat 2(E-M) 3.5m x 1.4m	Cat 3(P-M) 3.5m x 1.8m	Cat 4(P-P) 3.5m x 1.8m
7m	6.740	1.590	1.090	1.520
9m	4.631	1.312	1.321	1.314
10.5m	2.060	1.170	1.510	1.230
12m	1.710	1.160	1.510	1.200

Table 5a – Actual values of  $\rho_\phi$  denoted as resulting from pushover analysis (at failure) for version/trial 1 of the sixteen investigated bridge schemes. (Trial 1 corresponds to strict EC8-based design without reinforcement alteration/optimization)

Short pier Height	Cat 1(E-P) 3.5m x 1.4m	Cat 2(E-M) 3.5m x 1.4m	Cat 3(P-M) 3.5m x 1.8m	Cat 4(P-P) 3.5m x 1.8m
7m	1.180	1.010	1.010	1.520
9m	1.093	1.020	1.014	1.266
10.5m	1.110	1.034	1.100	1.220
12m	1.050	1.040	1.420	1.120

Table 5b – Actual values of  $\rho_\phi$  at failure (pushover analysis) for all investigated bridge schemes with optimized reinforcement ratios (Table 4a).

## 6. TIME HISTORY ANALYSIS

A series of 7 real earthquake records have been used and incrementally scaled up in terms of the spectral acceleration at the fundamental period of vibration of the subject bridge scheme to cover various seismic demands ranging from design level earthquake, passing through limit of elastic response until reaching failure of the bridge under investigation as per the failure criteria previously stated. Each earthquake has a different behavior and effect on each bridge, but the overall behavior will be reported in what follows only based on average results of the seven records. The earthquakes considered are LP89CAP, LP89G03, LP89HDA, NR94NYA, NR94STC, SF71PEL, and SH87WSM – refer to figure 6 showing records acceleration elastic response spectra. These records were extensively used in several other earlier studies (e.g. [12 & 14 – 17]) to which the reader is referred for complete details.

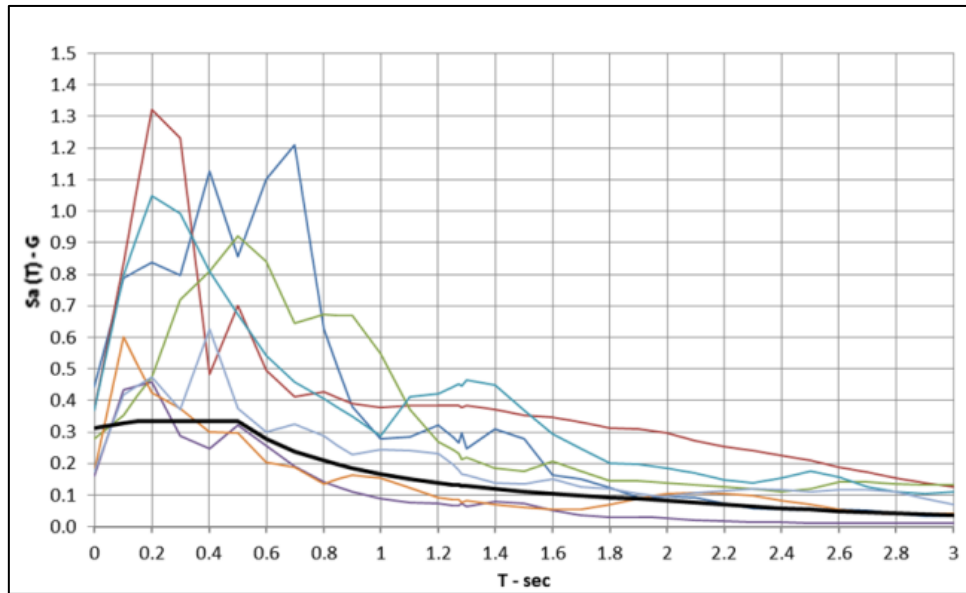


Figure 6 – Design acceleration response spectrum according to EC8 ( $q=3.5$ ) in Bold, compared to the seven earthquakes elastic response spectra before re-scaling them to design level.

The bridge piers undergo a typical moment-curvature hysteretic loop under inelastic time history analysis until either the end of the event or when failure is imminent at the stress-strain level of confined concrete and/or reinforcing bars as described before. The values of curvature at failure are determined according to failure criteria previously mentioned. Figure 7 displays a typical moment-curvature hysteretic loop for a sample bridge pier.

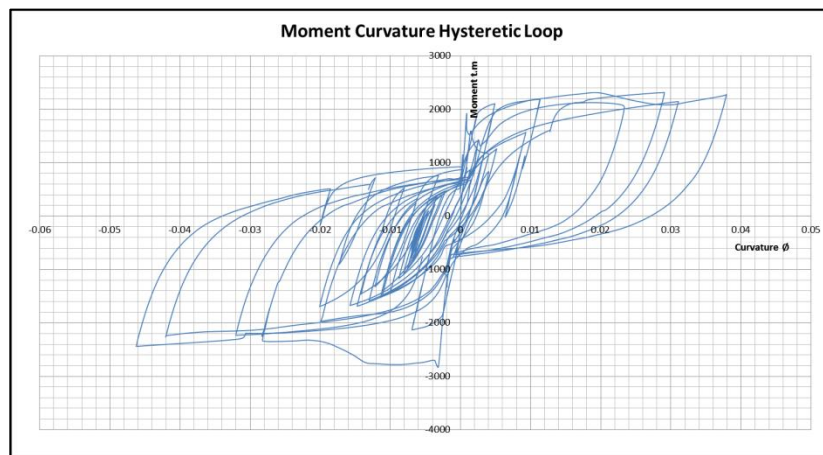


Figure 7 – Sample bridge pier Moment-Curvature hysteretic loop from time history analysis

## 6.1 CATEGORY 1 TIME HISTORY ANALYSIS RESULTS

In category 1, short pier behavior is influenced by the elastomeric bearing connection to the deck. Thus it is noticed that failure is governed by deck total displacement exceeding a seating width of 1m at abutment. This – of course – occurs after a “weak/soft” mode of failure (as previously defined) takes place, where net transverse shear deformation in the elastomeric bearing exceeds a maximum value of 0.45 m (refer to figure 8) for bridges with 7m or 9m-high short piers. Steel reinforcement strain values corresponding to this failure state are far

less than the maximum strain demarking failure of reinforcement. Average of the maximum achieved stress-strain values for the seven considered earthquake records is denoted in figure 9.

Concrete stress-strain relation to incrementing earthquakes is not shown since concrete strain values retrieved from inelastic time history analyses were far below maximum allowed strain values up to failure state of all studied bridges falling under this category 1. Most achievable bridge uniform behavior from various trials through altering reinforcement ratio of the short pier has resulted in much better performance than the original code-based design (table 2) previously denoted by trial 1. This difference is more obvious when comparing values of back calculated curvature-based  $\rho_\phi$  at failure (averaged over the seven considered earthquake records) as shown in figure 10 to those of the original EC8-based design (retrieved from pushover analysis and corresponding to trial 1) illustrated in table 5a.

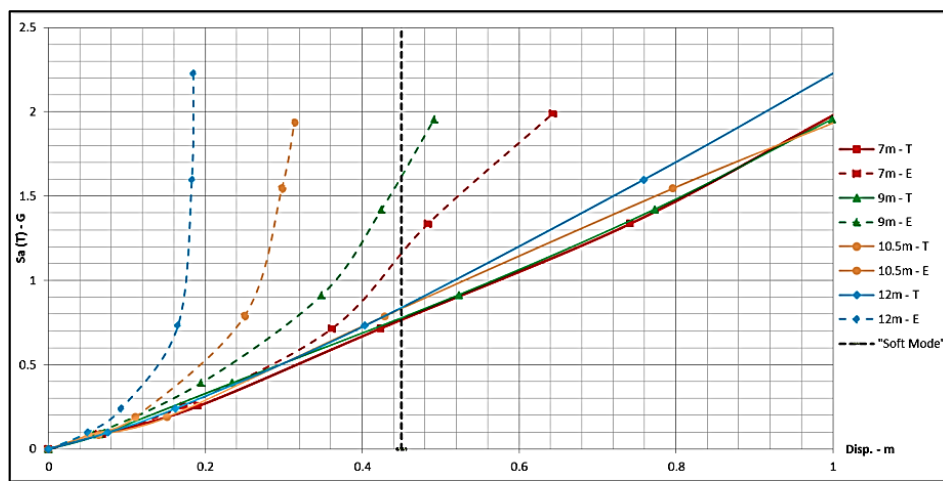


Figure 8 – Net elastomeric bearing displacement (E) and Total deck displacement (T) of all category 1 bridges. Values in the figure are average of the seven selected records.

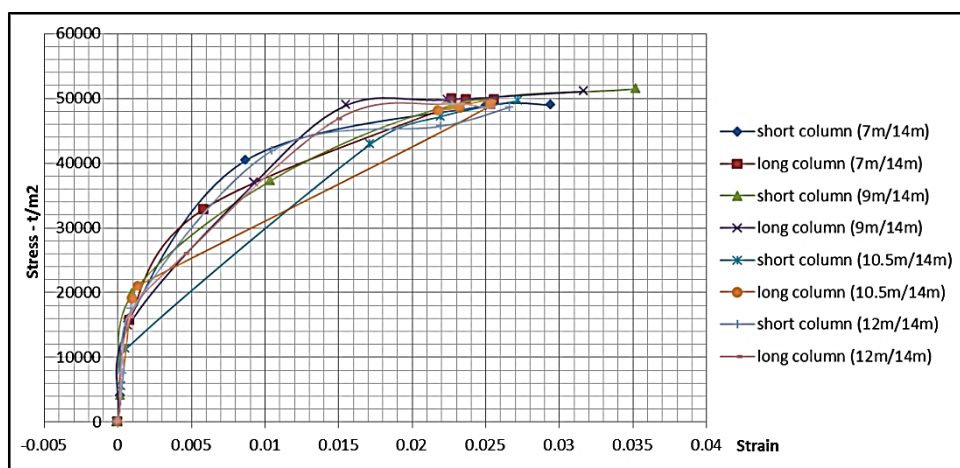


Figure 9 – Maximum stress-strain values resulting from increasing earthquake scale factor until failure – averaged over all seven earthquake records considered.

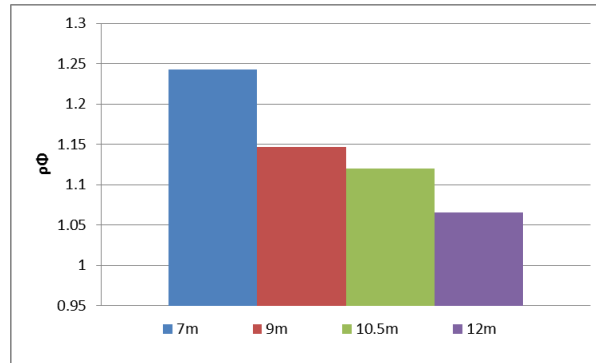


Figure 10 – Uniformity index, curvature-based,  $\rho_\phi$  for category 1 at failure for the four different heights of the short pier after optimizing EC8 original design through reinforcement ratio alteration (Table 4a) – reported values are averaged over the seven considered earthquake records.

An over strength value  $\Omega_R$  of the bridge is introduced and is defined as the ratio between the actual total base shear of the two piers at *failure level* resulting from time history inelastic analysis averaged over all seven considered earthquake records and the total design base shear of both bridge piers according to EC8 *design* response spectrum. The over strength  $\Omega_R$  (computed at failure limit state) of the bridge tends to decrease as the ratio between the height of the long to short piers decreases as shown in figure 11 (i.e., when piers tend to be of near height). Similarly, another strength response index denoted by  $\Omega_d$  is defined and computed but at the *design demand* level rather than at the failure level.  $\Omega_d$  is simply defined as the total base shear carried by both unequal height piers (averaged over the seven considered earthquakes) corresponding to the design level demand divided by the base shear the actual bridge piers are designed for in order to sustain EC8 seismic demands. As the value of  $\Omega_d$  decreases and is less than 1.0, the as-designed bridge has higher design strength than expected. On the other hand, when the value of  $\Omega_d$  becomes greater than 1.0, the bridge as-designed is exposed to actual earthquake forces at *design level* higher than its design ability to resist. Referring to figure 11, it is clear that the case study bridges of category 1 are all featuring  $\Omega_d$  remarkably less than 1.0 irrespective of the ratio of their unequal height piers. They thus feature a reasonable built-in over strength and are hence *on average* capable of sustaining EC8 seismic design loads when hit by design level earthquake records.

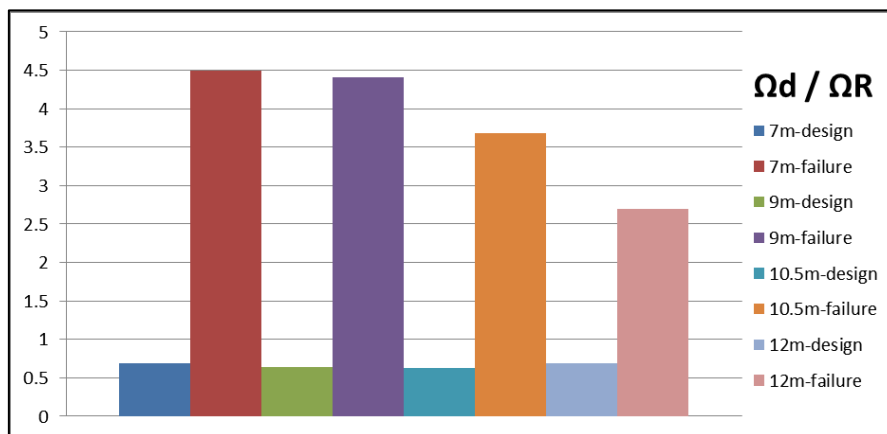


Figure 11 – Over strength values ( $\Omega_d$  at design level and  $\Omega_R$  at failure level) retrieved averaged over all considered seven earthquake records for category 1 bridges – design data are as per Table 4a.

## 6.2 CATEGORY 2 BRIDGE BEHAVIOR

Category 2 is distinguished from category 1 at many features. First of all, the bounding failure criteria here is the ultimate steel strain as opposed to maximum deck displacement and off-seating as shown in figures 12 and 13. The total deck displacement has never exceeded the preset seating width of 1m and the net elastomeric bearing transverse shear deformation has not reached the weak mode of failure demarcated by elastomer shear deformation of  $3x t_b$ .

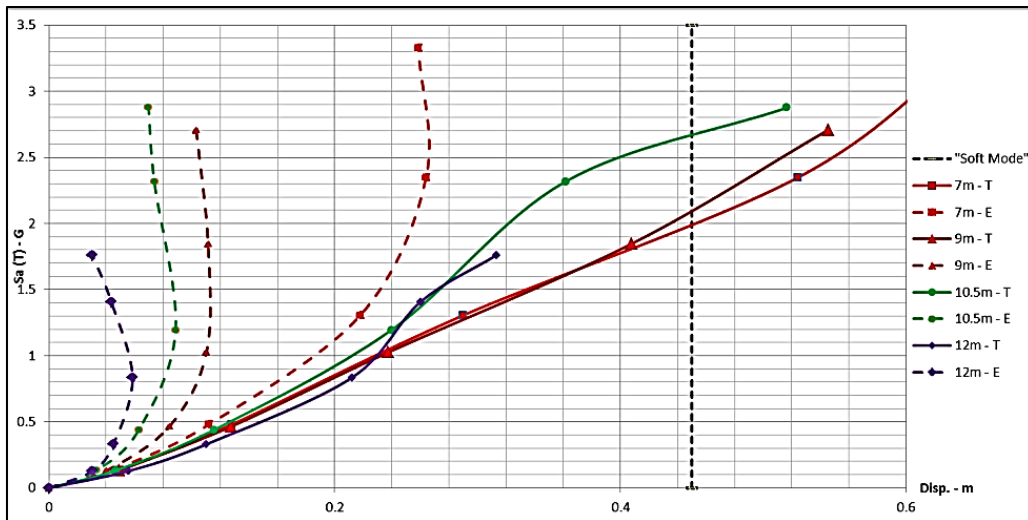


Figure 12 – Net elastomeric bearing displacement (E) and Total deck displacement (T) of all category 2 bridges. Values in the figure are average of the seven selected records.

Steel strain controlled failure mode is governing all studied bridges of this category, as in most notable cases short pier tends to fail first for heights 7m and 9m while this effect diminishes whenever we approach cases with close pier heights, i.e., 12 m-high short pier (refer to figure 13).

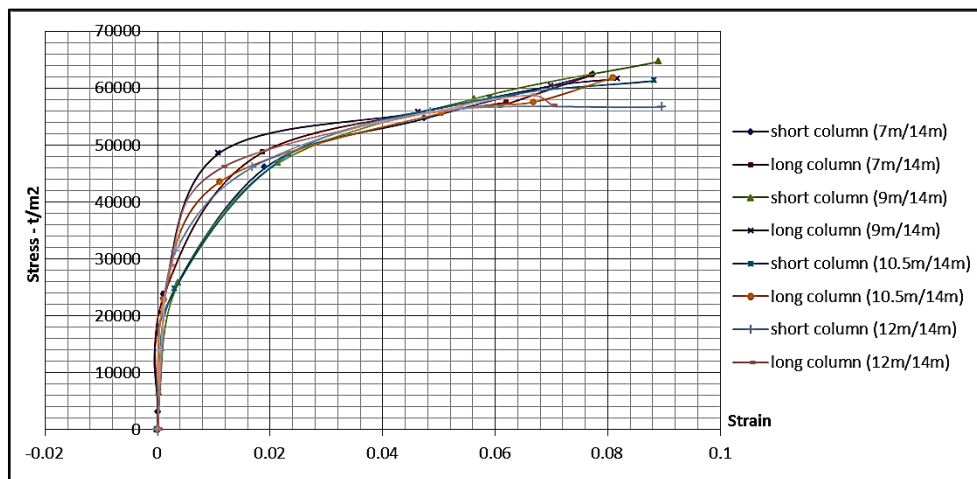


Figure 13 – Maximum stress-strain values resulting from increasing earthquake scale factor until failure of category 2 bridges – averaged over all seven earthquake records considered.

From a seismic response uniformity/regularity perspective, category 2 bridges possess less uniform behavior – especially at failure – than category 1. One can also note that there is a



reversal in behavior in terms of uniformity (and synchronized failure of unequal height piers) when short pier height exceeds 9m. In other words, the scheme with 12m-high short pier possesses low uniformity behavior nearly similar to the scheme with the 7m-high short pier already featuring some inherent non-uniform seismic behavior particularly at failure (refer to figure 14). This is due to some intrinsic effect of monolithic pier-to-deck connection. To conclude, when we have bridge schemes with close heights of piers, it is recommended to consider category 1 instead as its inherent features provide overall better uniformity in seismic response than category 2.

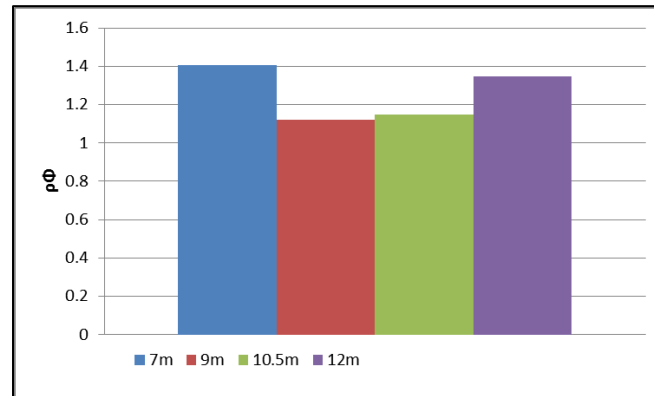


Figure 14 – Uniformity index, curvature-based,  $\rho\phi$  for category 2 at failure for the four different heights of the short pier after optimizing EC8 original design through reinforcement ratio alteration (Table 4a) – reported values are averaged over the seven considered earthquake records

Regarding built-in over strength, category 2 bridges possess lower over strength at failure than their corresponding versions of category 1 as reflected by  $\Omega_R$  values in figure 15 versus figure 11, while they possess critical values of *design* strength index,  $\Omega_d$  that are very close to 1.0 which denotes that these bridges – as-designed – can sharply withstand design earthquakes.

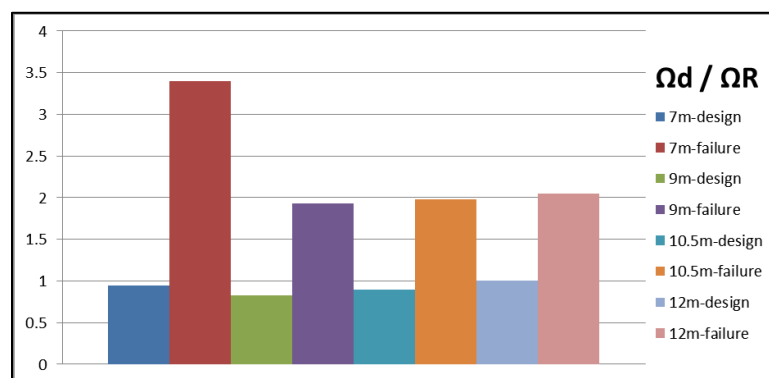


Figure 15 – Over strength values ( $\Omega_d$  at design level and  $\Omega_R$  at failure level) retrieved averaged over all considered seven earthquake records for Category 2 bridges – design data are as per Table 4a.

## 7. MATERIAL ECONOMY AMONG CATEGORY 1 AND CATEGORY 2

Material economy - besides uniformity of seismic response and over strength (both at design and at failure states) - plays a key role in determining the most suitable system according to the available scheme conditions. The designer may sometimes favor bridge material economy over uniformity of behavior. To unify a measurement technique to address and assess the economy of the as-designed bridge,  $\beta_c$  and  $\beta_s$  are two proposed *dimensional* indexes deemed suitable to compare various studied bridge schemes in terms of concrete and reinforcing steel quantities, respectively.

$$\beta_c = \frac{\text{Total base shear force}}{\text{Total piers cross section area}}, \quad \beta_s = \frac{\text{Total base shear force}}{\text{Total reinforcement area in both piers}} \quad (\text{t/m}^2) \quad (3)$$

These indexes ignore piers height and are hence used only to compare similar bridge schemes but with different pier-to-deck connections. Higher values of  $\beta$  means better material economy, since higher forces can be sustained for a given quantity of material (be it concrete or reinforcing steel). However, high  $\beta$  values do not necessarily illustrate a better design in terms of uniformity of seismic behavior, redundancy and/or over strength capability. Figures 16a and b denote a comparison between category 1 and category 2 bridges in terms of economy and material utilization.

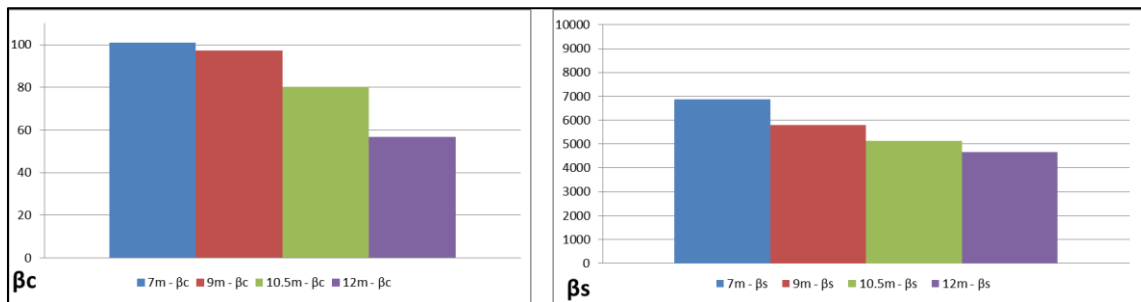
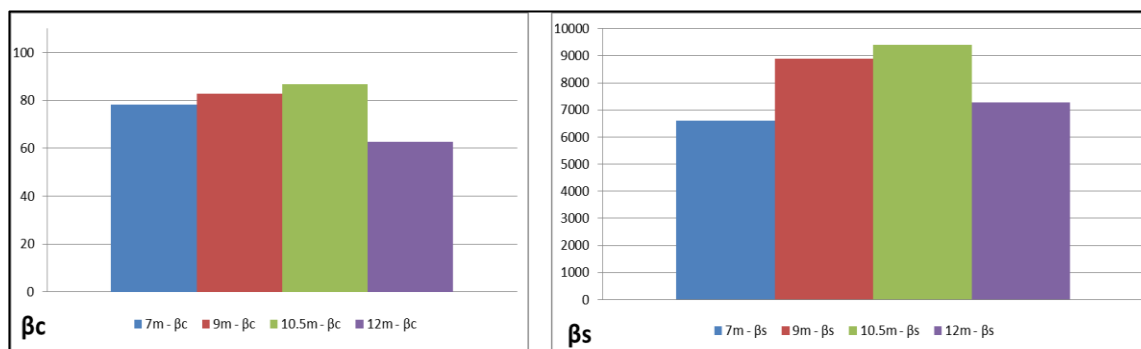


Figure 16a –  $\beta_c$  and  $\beta_s$  for category 1 bridges – averaged over the seven selected records



.Figure 16b –  $\beta_c$  and  $\beta_s$  for category 2 bridges – averaged over the seven selected records.

It is obvious that in terms of better concrete utilization, category 1 outnumbers category 2 just for bridge schemes with short pier heights of 7m and 9m (i.e., remarkably different from the height of the longer pier that is 14m), but both categories possess nearly same utilization

for short pier heights of 10.5m and 12m. In terms of steel utilization and excluding short pier of height 7m, category 2 far outnumbers category 1 which denotes that steel reinforcement used in category 2 sustains much more shear force than reinforcement used in category 1. It is worth noting that values in figure 16 reflect results averaged over the seven selected earthquake records and correspond to bridge schemes with steel reinforcement ratios tailored to comprehend best achievable uniform behavior as per table 4a.

## 8. CONCLUSIONS

Current EC8 criteria in addressing bridge uniformity shall hold further investigation, as the only factor to determine uniformity ( $\rho < 2$ ) is force/moment-based and hence is not enough to assess actual bridge behavior and might be misleading in some cases as discussed herein and in the literature. A curvature-based uniformity index such as  $\rho_\phi$  proposed in the present research has been shown to be more appropriate to address and verify this seismic regularity issue for bridges.

Common construction practice might force designers to choose one type of bearing to be used across bridge piers, which is good from aesthetic point of view and constructability but may be a bad option in terms of design optimization targeting utmost uniformity of seismic response. For instance, pot bearings when used on all piers of the same bridge irrespective of their relative height could lead to *less* economic and/or *less* effective design to overcome seismic loads for one case or the other, while still providing *some* uniform behavior among unequal height bridge piers (refer to tables 4b and 5b). Further altering pier-to-deck connections can provide better uniform behavior. Such conclusion based on pushover analysis results is under further investigation by the authors through applying more sophisticated inelastic time history analyses.

Usage of elastomeric bearing on short pier and pot bearing on long pier possesses an effective solution for bridge uniformity under seismic events up to failure in addition to overall material optimized utilization. On the other hand, usage of monolithic connection instead of pot bearing for the long pier is not recommended, as it sustains low over strength characteristics although it still offers uniform seismic behavior close to that provided through the pot bearing solution.

In the case with elastomeric bearing on the short pier, concrete usage economy is better when pot bearing is mounted on long pier, especially when the gap between pier heights is large. But when both piers have closer heights, the monolithic pier-to-deck connection for the long pier along with elastomeric bearing on the short pier shows slightly better concrete utilization. Also, the monolithic connection possesses generally much higher steel reinforcement utilization than the pot bearing pier-to-deck connection for the long pier except for the bridge schemes with 7m-high short pier. However, this benefit effect is diminished when comparing this scheme to the pot bearing connection scheme in terms of seismic behavior uniformity and over strength.

Finally, usage of pot bearings on both piers is not highly recommended, same as usage of pot bearing on short pier and monolithic connection for long pier. Both schemes show very rigid solution attracting significantly higher seismic demands, and may have unexpected “*hard to minimize*” non-uniform seismic behavior. Nonetheless, further extensive investigations through inelastic time history analysis are a must to determine their exact behavior and to weigh their effectiveness in terms of regularity/uniformity of seismic

response, in addition to their built-in overstrength, versus quantities of structural materials (concrete and reinforcement steel) used. This is currently an ongoing research by the authors.

## ACKNOWLEDGMENTS

The research reported here was supported by the European Union Project PIRSES-GA-2010-269222: Analysis and Design of Earthquake Resistant Structures (ADERS) of the FP7-PEOPLE-2010-IRSES, Marie Curie Actions. This support is gratefully acknowledged by the authors.

## REFERENCES

- [1] EN 1998-1 Eurocode 8 (2005): "Design of Structures for Earthquake Resistance. Part 1: General Rules, Seismic Actions and Rules for Buildings," *Comité Européen de Normalisation*, Brussels, Belgium.
- [2] EN 1998-2 Eurocode 8 (2005) "Design of Structures for Earthquake Resistance, Part 2: Bridges," *Comité Européen de Normalisation*, Brussels, Belgium.
- [3] Guirguis, J.E.B. and Mehanny, S.S.F. (2013), "Evaluating Codes Criteria for Regular Seismic Behavior of Continuous Concrete Box Girder Bridges with Unequal Height Piers," *ASCE Journal of Bridge Engineering*, DOI 10.1061/(ASCE)BE.1943-5592.0000383, Vol. 18, No. 6, June 2013, pp 486-498.
- [4] Mohammadi-Tamanani, M and Ayoub, A. (2014), "Design of Bridges with Unequal Pier Heights," *Structures Congress*, Boston, Massachusetts, USA April 3-5, 2014.
- [5] Reza, S.M. (2012), "Seismic Performance of Multi-Span RC Bridge with Irregular Column Heights," *Master of Applied Science Thesis*, The University of British Columbia, Canada.
- [6] Tehrani, P. (2012), "Seismic Analysis and Behavior of Continuous Reinforced Concrete Bridges," *Ph.D. Thesis*, McGill University, Montreal, Quebec, Canada.
- [7] OpenSees 2.0.0 [Computer software]. Berkeley, CA, Pacific Earthq. Engrg. Res. Center, Univ. of California.
- [8] Caltrans (SDC) Seismic Design Criteria, Version 1.7 - September 2013.
- [9] South Carolina Department of Transportation (SCDOT). (2008). "Seismic Design Specifications for Highway Bridges," version 2.0, SCDOT, Columbia, SC.
- [10] Konstantinidis, D., Kelly, J.M. and Makris, N (2009), "Experimental Investigation of the Seismic Response of Bridge Bearings", 3rd International Conference on Advances in Experimental Structural Engineering, San Francisco, CA, 15-16 October, 2009 Manos et al. (2011)
- [11] Manos, G.C., Mitoulis, S.A. and Sextos, A.G. (2011), "Preliminary Design of Seismically Isolated R/C Highway Overpasses – Features of Relevant Software and Experimental Testing of Elastomeric Bearings," COMPDYN 2011, III ECCOMAS Thematic Conference on Computational Methods in Structural Dynamics and Earthquake Engineering, Corfu, Greece, 26-28 May, 2011.

- [12] Farag, M.M.N., Mehanny, S.S.F. and Bakhoun, M.M. (2015), "Establishing optimal gap size for precast beam bridges with a buffer-gap-elastomeric bearings system" *Earthquakes and Structures*, accepted for publication.
- [13] EN 1992-1-1 Eurocode 2 (2004), "Design of Concrete Structures. Part 1-1: General Rules and Rules for Buildings," *Comité Européen de Normalisation*, Brussels, Belgium.
- [14] Mehanny, S.S.F. (2009), "A Broad-Range Power-Law Form Scalar-Based Seismic Intensity Measure," *Engineering Structures*, Vol. 31, Issue 7, pages 1354-1368, July 2009.
- [15] Chenouda, M. and Ayoub, A. (2009), "Probabilistic collapse analysis of degrading multi degree of freedom structures under earthquake excitation," *Eng. Struct.* 2009; 31(12), pp. 2909-2921.
- [16] Mehanny, S.S.F., and Ayoub, A.S. (2008), "Variability in Inelastic Displacement Demands: Uncertainty in System Parameters versus Randomness in Ground Records," *Engineering Structures*; 30(4): 1002-1013.
- [17] Mackie K.R. and Stojadinović B. (2005), "Fragility Basis for California Highway Overpass Bridge Seismic Decision Making," *PEER Report 2005/02*, University of California, Berkeley, CA, USA.